J. Earth Syst. Sci. (2020)129 86
https://doi.org/10.1007/s12040-019-1337-9

Tectonic evolution of Kutch sedimentary basin, western India

K Chandra Mouli[1], P Chandrasekhar[1,*], D P Rao[1] and V K Dadhwal[2]

[1]*National Remote Sensing Centre, Indian Space Research Organisation, Hyderabad 500 037, India.*
[2]*Indian Institute of Space Science and Technology (IIST), Thiruvananthapuram 695 547, India.*
**Corresponding author. e-mail: chandrasekharpatibandla@gmail.com*

MS received 8 July 2019; revised 1 November 2019; accepted 15 November 2019

Lithological variations, circular spectral anomalies, geological structures such as folds, faults, lineaments and shear zones of Kutch sedimentary basin were interpreted using IRS-LISS III satellite data. Aeromagnetic data was also interpreted qualitatively and quantitatively and a number of anomalous magnetic zones, faults, lineaments and domal structures were mapped. Magnetic basement depths and thickness of sediments were also computed. A number of alternate basement ridges/highs/uplifted blocks and depressions/lows/downthrown blocks were delineated. The information obtained from satellite remote sensing and aeromagnetic data were then integrated and the results were compared with published literature on gravity, magnetic (ground), magnetotelluric and seismic data, and also with field geology and well data. Structural controls in spatial domain (latitude, longitude and depth) were derived by establishing spatial relationship among different geological structures with reference to the geological time scale. Numerous horst and graben structures (ridges and sub-basins) as well as a number of master faults were delineated which serve as vital information with regard to hydrocarbon prospects and earthquake vulnerability, respectively. Based on the information obtained from this integrated study, a conceptual tectonometamorphic model along with sedimentation and igneous activity (ophiolitic and basaltic) has been constructed which has a significant bearing on the sequence of events that occurred during the deformational history of Kutch sedimentary basin resulting into the present day tectonic configuration.

Keywords. Fold; fault; lineament; IRS-LISS III satellite data; aeromagnetic data; tectonic configuration.

1. Introduction

Regional geological understanding is essentially required not only for the exploration and exploitation of natural resources but also for theoretical/research/modelling purpose. Conventionally, geological mapping is done by carrying out field survey based on the observation of rock exposures, analysis of the vertical sections of earth cuttings and well logs. The advent of remote sensing technology employing satellites as the most common platforms for collection of data has brought in significant changes in geological mapping. Multispectral sensors onboard satellites provide images of high quality having huge potential for mapping lithology, geological structures such as folds, faults, fractures, lineaments and shear zones and geomorphology, which serve as the vital information in the context of geological exploration (Rao *et al.* 1992, 1996; Chandrasekhar *et al.* 2009, 2011; Sreedhar Ganapuram *et al.* 2009; Chandrasekhar 2010; Masoud and Koike 2011;

Published online: 04 March 2020

Seshadri and Chandrasekhar 2013; Ganguly and Mitran 2016; Seshavataram 2016; Al-Nahmi *et al.* 2017; Thakkar 2017; Das *et al.* 2018). This is possible because of the synoptic view offered by the satellite imagery and the unique capability of establishing spatial relationship among different geological/structural features. On the other hand, the utility of aeromagnetic data for geoscientific applications and research studies was discussed at length, demonstrated and documented by several authors over the last few decades (Rama Rao and Murthy 1978; Hinze and Zietz 1985; Reddy *et al.* 1988; Reid *et al.* 1990; Cowan and Cowan 1991; Zonenshain *et al.* 1991; Reeves 1992, 1994; Blakely 1995; Mathew *et al.* 2001; Ramachandra *et al.* 2001; Anand and Rajaram 2002; Prasanti Lakshmi and Ram Babu 2002; Rajaram Mita and Anand 2003; Colin Reeves 2005; Rajaram *et al.* 2006; Rajendra Sarma *et al.* 2006; Murthy 2007; Aitken and Betts 2008; Akintayo *et al.* 2014; Chandrasekhar *et al.* 2018). Integrated interpretation of the above two data sets would yield reliable information on the surface as well as the subsurface geology, structure and tectonics (Chandrasekhar *et al.* 2011; Chandrasekhar and Seshadri 2013).

The sedimentary basin of Kutch in Gujarat state has a great economic and tectonic significance in terms of oil and gas reserves (Seshavataram 2016; http://www.dghindia.org/17.aspx; https://www.google.co.in/?gfe_rd=cr&ei=TDJ5VcuuCerI8AeLrLmoCg&gws_rd=ssl#q=Kutch++geological+maps) and earthquake vulnerability (http://www.imd.gov.in/section/seismo/static/seismo-zone.htm), respectively. This region falls in Zone V of the Seismic Zonation Map of India (http://www.imd.gov.in/section/seismo/static/seismo-zone.htm) indicating highest risk for earthquake occurrence and is the only such zone outside the Himalayan seismic belt in India. Hence, a thorough understanding of the subsurface geological structure, deformational history and the tectonics of the basin is an essentially required scientific outcome. Kutch is a western marginal pericratonic rift basin in India that is oriented E–W at the periphery of the Indian Craton. This region is geologically well known for its Mesozoic and Tertiary sedimentation over the crystalline basement and also vulnerable for earthquake occurrence and hence is extensively studied by a number of researchers in the past (Biswas 1971, 1974, 1981, 1982, 2005, 2012; Biswas and Deshpande 1973, 1970, 1968; Deshpande 1982; Sylvester 1988; Merh 1995; NRSA Tech Rep 1998; Ravi Shanker 2001; Kusala Rajendran *et al.* 2001; Gaonkar 2003; Sumer Chopra *et al.* 2010; Seshavataram 2016; Thakkar and Amal Kar 2017; Chandrasekhar *et al.* 2018). Lithological sequence and major geological structures like faults and fold systems were mapped by geological and geophysical investigations and reported in the above literature. Few major structural zones surrounding and within Kutch region were also named.

Therefore, in the process of studying Kutch basin, enormous wealth of geoscientific information has been generated and documented. The early works were primarily based on theoretical models, field geological surveys and ground geophysical investigations. The studies based on theoretical models could bring out major sets of faults and their intersections. Geological surveys on ground could also map only a limited number of structures such as major faults, few lineaments and parts of lineaments/structures. All the lineaments and structures could not be mapped during field surveys, perhaps as they get obscured by soil/vegetation cover. Hence, the continuity of faults, their intersection and the relationship with other geological features could not be established. Geophysical investigations such as gravity, magnetic (ground), magnetotelluric and seismic methods of prospecting were also conducted in Kutch basin. As these methods are ground-based, the data was acquired along the available road networks. As a result, the geophysical coverage is non-uniform. Hence, the geoscientific information generated so far is inadequate to explain the subsurface geological structure and tectonic framework of the basin to the required details of constructing a subsurface geological model. Therefore, an attempt is made in the present study to interpret space-borne IRS-LISS III and airborne magnetic data by mapping basement structures and computing sediment thickness, for the first time, having complete and uniform coverage for the whole basin and to integrate the results for generation of a conceptual tectonometamorphic model, which can explain the sequence of events that could have triggered in the poly-phase deformational history of the basin resulting into the present day horst and graben structures hosting huge Tertiary and Mesozoic sedimentation.

2. Geology and physiography

The stratigraphy of Kutch basin comprises strata ranging in age from Lower Jurassic to Holocene and the complete sequence is exposed only in the

Kutch mainland (Biswas and Deshpande 1970; figure 1). The older Mesozoic sequence is exposed in Pachham, Khadir, Bela and Chorar islands to the north of Kutch mainland, whereas the strata of intermediate age of Mesozoic sequence are in the 'Wagad Highland'. The Tertiary rocks are exposed in the peripheral plains of these 'Highlands'. Palaeocene (Palaeogene) rocks are deposited mainly in the southwestern coastal plains of Kutch mainland whereas Neocene (Neogene) rocks extend into much interior crossing the eastern boundary of the basin. The extensive flows of Deccan Traps representing volcanic activity in this region had terminated the Mesozoic sedimentation during Late Cretaceous to Early Palaeocene times (Biswas 1982). The Kutch region consists of the embayment between Nagar Parkar uplift in north, Kathiawar uplift in south, Radhanpur–Barmer arch in east and a sloping platform featured by parallel E–W oriented uplifts (Highlands/Islands) at the center, surrounded by 'residual depressions' (plains of Great and Little Rann). Six major uplifts namely, Pachham, Khadir, Bela islands, Chorar hills, Wagad highlands and Kutch mainland occur in three sub-parallel trending E–W lines (Biswas 1982; Ravi Shanker 2001). The basin is filled up with sediments ranging in age from Middle Jurassic to Holocene. Deccan Trap lava flows of Late Cretaceous to Early Palaeocene age divide the Mesozoic and Tertiary stratigraphy of the Kutch region (http://www.jsce.or.jp/report/12/Indian/Report/PDF/indo3.pdf).

All the hill ranges and the intervening low grounds of Kutch region run almost parallel, which is the characteristic feature indicating that the topography is controlled by the geological factors such as folding, faulting and lithology to a larger extent.

3. Methodology

Indian Remote Sensing Satellite (IRS 1C) data of LISS III sensor having 23.5 m spatial resolution has been procured from the National Remote Sensing Centre (NRSC) Data Centre (NDC) of the Indian Space Research Organisation (ISRO) in digital format (as a part of the project work for Directorate General of Hydrocarbons (DGH), New Delhi) for carrying out the geological interpretation of Kutch basin (http://bhuvan.nrsc.gov.in). The raw data was mosaiced for clipping the boundaries of the study area and geo-rectified with the help of topographic maps. Image enhancement techniques such as linear stretch, edge enhancement and haze removal were applied to the raw data for feature extraction. Resistant formations usually form prominent ridges because of their resistance to erosion. The acidic rocks/sedimentary rocks show brighter tone and have distinct appearance, whereas the mafic rocks are manifested in darker tone. The carbonates–carbonate facies rocks and meta-argillites exhibit darker tone in relatively low lying areas. Different rock types were distinguished and mapped based on their diagnostic spectral signatures, as

Stratigraphic sequence

Coastal sands, Mud flats, Rann sediments, Alluvium, Residual deposits – Holocene

Miliolite (Aeolian)	- Pleistocene
Marine to Fluviomarine beds	- Eocene to Pliocene
------------Unconformity------------	
Laterite	- Palaeocene
Basalt and associated intrusive massive rocks	- Upper Cretaceous to Palaeocene
------------Unconformity------------	
Marine to Fluviomarine beds	- Lower Jurassic to Middle Cretaceous
------------Unconformity------------	
Basement	- Archaean and Proterozoic

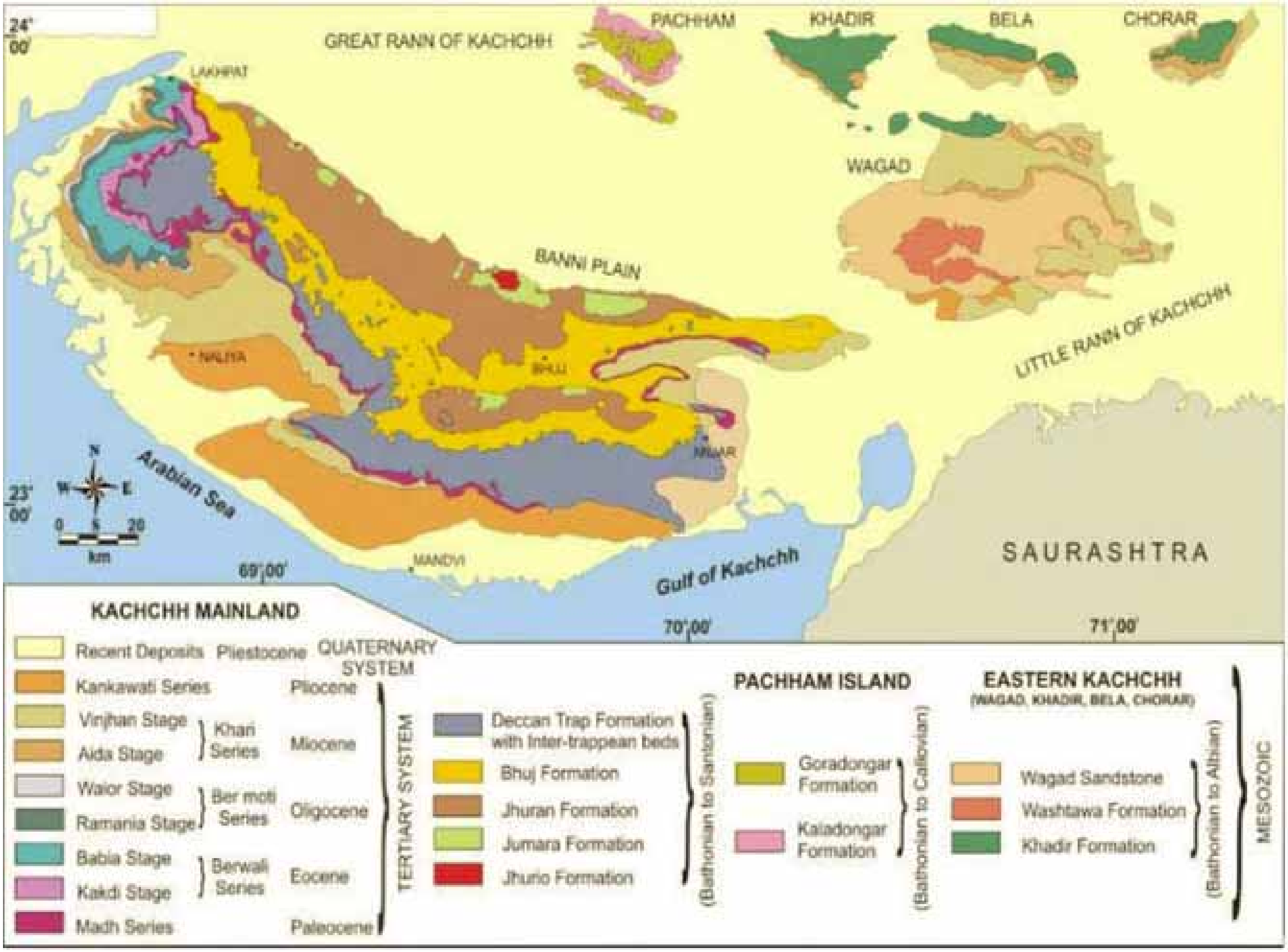

Figure 1. Geological map of the study area (source: Biswas and Deshpande 1970).

the electromagnetic signal is sensitive to the composition and form of a rock type. Subsequently, other geological features such as folds, faults and lineaments were interpreted based on the image elements such as tone, texture, pattern, association, shape, size and shadow and the geotechnical (terrain) elements such as land use, land cover, vegetation and drainage. 'Faults' were interpreted from satellite data based on the anomalous truncations or offsets of formations, sharp topographic breaks (linear scarp faces), dislocations of the linear anomaly trends, alluvial fans and alluvial cones along linear scarp face and abrupt truncation of fold patterns along a line (Mikhailov 1987; An and Sammis 1996) whereas 'lineaments' were interpreted as anomalous features due to their characteristic tonal variations, spatial relationship with other geological units and linear alignment of streams/water bodies/vegetation. The geomorphic anomalies appearing in the form of folded structures were interpreted based on the identification of trends of anomalies, trend lines, tone and drainage pattern. Numerous curvilinear anomalies, fold patterns and circular spectral anomalies were also mapped from satellite data based on terrain morphology, tonal variations, smooth texture and drainage anomalies. Geological interpretation of IRS-LISS III data is presented in figure 2. The data processing, analysis and interpretation of satellite data was carried out using PCI-GEOMATICA and ERDAS IMAGINE softwares.

The regional aeromagnetic data flown at an altitude of 5000 ft above mean sea level by NRSC/ISRO for DGH along N–S flights with a flight line spacing of 2000 m was used in the present study. Diurnal corrections were applied to the onboard data by selecting the appropriate reference magnetic level. The differences in the magnetic field values at the points of intersection of each of the tie lines with those of the flight lines were then corrected during tie-line corrections for removing the effects of monthly shift in magnetic levels and the residuals leftover after diurnal corrections. Tie-line corrected data was then corrected for the earth's model field, i.e., International Geomagnetic Reference Field (IGRF) for enhancing the crustal magnetic anomalies, gridded with a grid cell size of 400 m (1/5 of the

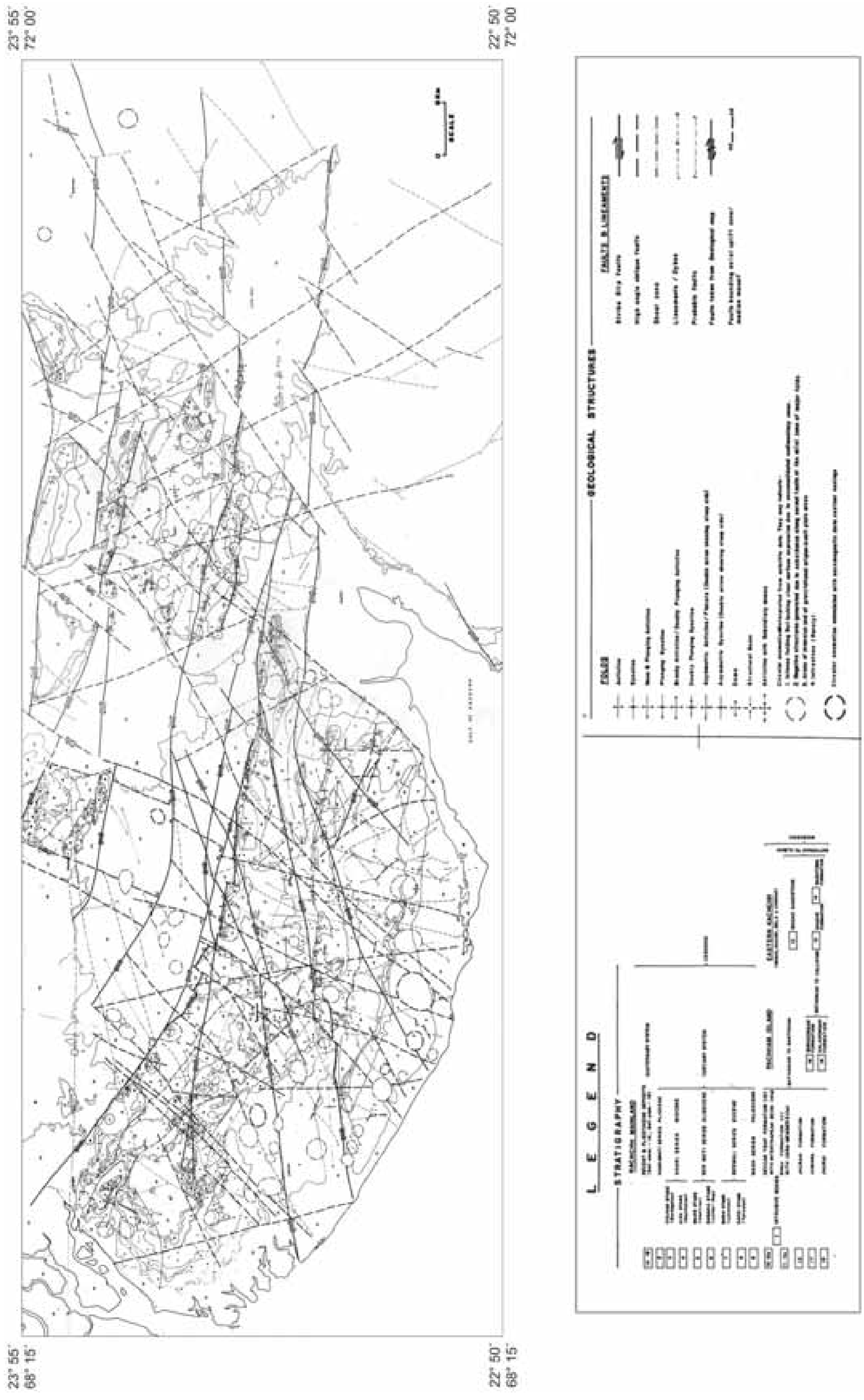

Figure 2. Geological structures and tectonic trends interpreted from IRS-LISS III satellite data.

flight line spacing) and contoured with a contour interval of 20 nT. IGRF corrected aeromagnetic images (grey image and pseudo colour image) were also generated for improved and reliable interpretation of the geological features (figure 3), as there is no limitation of contour interval when the data is in image form (Willian and Willian 1987; Suryanarayana *et al.* 1992; Milligan and Gunn 1997). As the aeromagnetic data comprises information from subsurface geological strata lying at different depths in the earth's interior and is reflected as a cumulative effect, the IGRF corrected data was then subjected to regional–residual separation and computation of second vertical derivatives (SVD) in order to emphasize the contributions of relatively shallow features as well as to resolve the overlapping anomalies (Boyd 1969; Babu Rao *et al.* 1987; Berger *et al.* 2004; Boyd and Isles 2007; Anudu *et al.* 2012). Dislocations of the linear anomaly trends or abrupt changes in the anomaly type and pattern or changes in the background level of the magnetic field were identified and used for demarcating 'faults'. The linear features without clear dislocations, magnetic gradients and alignment of anomalies were interpreted as 'magnetic trends' or 'lineaments'. Igneous intrusions usually produce domal structures in the sedimentary strata and all such 'intrusions' were identified by magnetic methods (Rama Rao and Murthy 1978; Ghosh and Ramesh Acharya 2006; David and Leigh 2013). Basement depths for each and every structure interpreted from aeromagnetic and remote sensing data as well as the same structure at different locations were also computed using aeromagnetic data by means of quantitative interpretation techniques (Rao and Babu 1984; Reid *et al.* 1990). Computed basement depths were also validated with the help of the interpretation software (Radhakrishna Murthy 1992) developed exclusively for the well-defined and unclustered magnetic anomalies and also with the well data provided by DGH during the project work. A number of alternate basement ridges/highs/uplifted blocks and depressions/lows/downthrown blocks were delineated (Chandrasekhar *et al.* 2018). The data processing, analysis and interpretation of aeromagnetic data were carried out using indigenously developed software of NRSC/ISRO.

The results obtained from the interpretation of satellite remote sensing (XY/spatial/lateral) and aeromagnetic data (Z/vertical/depth) were then

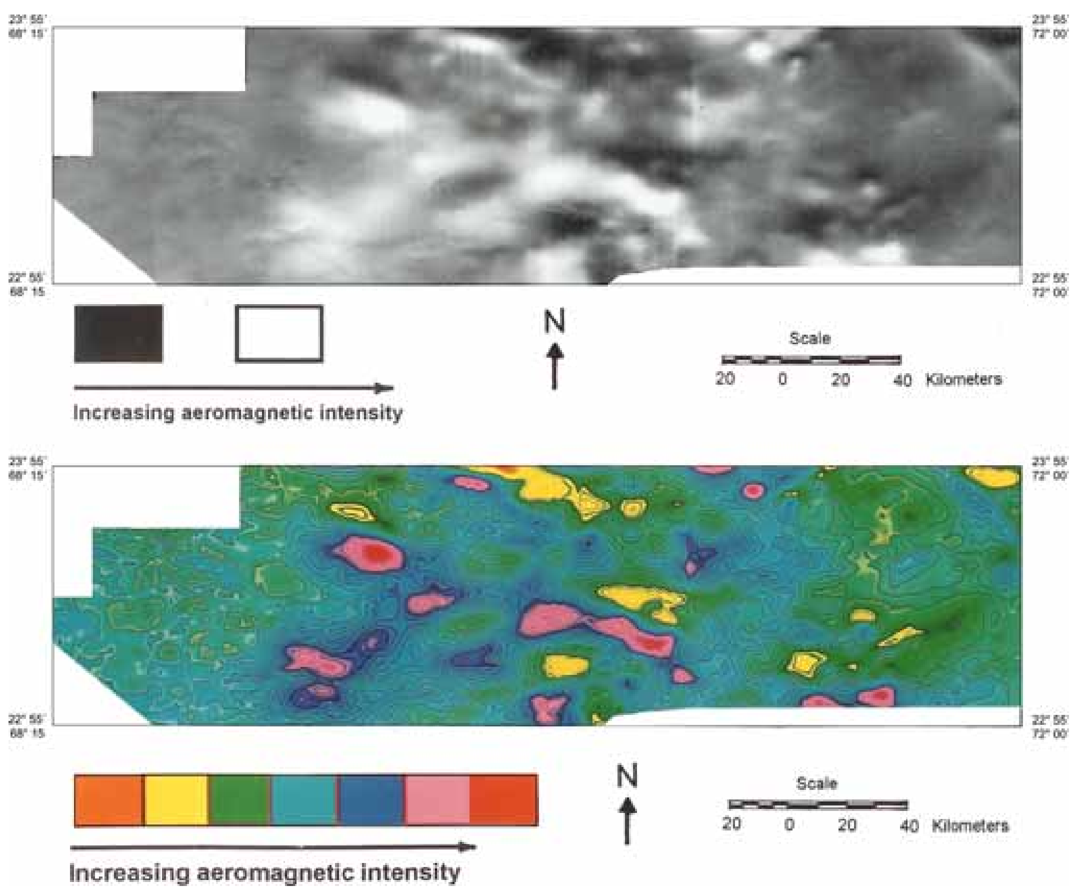

Figure 3. Aeromagnetic images of the study area: grey image (top); pseudo colour image (bottom).

Figure 4. Aeromagnetic (residual) contours and tectonic trends superimposed on IRS-LISS III satellite data.

integrated (figure 4) and analyzed in conjunction with the published literature on gravity, magnetic (ground), magnetotelluric and seismic data interpretation (Misra *et al.* 2003; Mishra *et al.* 2004, 2005; Chandrasekhar *et al.* 2005, 2011; Nagarjuna and Rao 2019). The methodology followed is presented in the form of a flowchart in figure 5.

4. Results and discussion

Kutch is a western marginal peri-cratonic rift basin that is oriented E–W at the periphery of the Indian Craton. All the possible geological structures (minor, major and mega) and litho units of the basin were mapped in this study, which could bring out a number of new geological features such as folds, faults, circular spectral anomalies and shear zones, and augmented existing geology significantly. Numerous horst and graben structures were also mapped by deriving the latitude, longitude and depth data, as mentioned above. Spatial analysis of all the above geological features was carried out and their inter-relationship and relative displacements were established. The basin configuration as observed from satellite data indicates a broad synclinal structure covering the whole sequence of rocks resting on the basement with its axial trace/uplift running in NE–SW direction. Two major faults were interpreted from satellite data (shown as AZ in figure 2). They are extending parallel to the direction of axial trace, from SW corner to NE corner, right up to Pacham island in the Kutch mainland region. They encompass centers of Mesozoic deposition, which are representative of median massif. Satellite data interpretation has brought out a new dimension that the median massif is also broadly segmented. The segmented uplifts were displaced and oriented in E–W direction, because of the effect of later strike-slip and thrust faults along the northern margin of Kutch mainland and further north. Later, this ancient platform is subjected to simple shear stress in NE–SW or ENE–WSW direction. The main characteristic feature of geosynclinal regime is reduction in areas and expansion of platforms. These crustal movements might have been conditioned by emplacement of magma, disturbances of isostatic equilibrium, displacements and rotation of large parts of this continent. The geological features interpreted from remote sensing and aeromagnetic data are genetically connected with linear folded and ruptural deformations (also supported by Mikhailov 1987; Chandrasekhar *et al.* 2005). The tectonic deformation had started with vast ancient platform of crustal region of gneissic rocks. The total structural framework is understood and explained in terms of development of the faulted, folded and ruptural structures in geosynclinal environment resulting in genetically connected horizontal and vertical movements, analysis of the mechanism of deformation in each stage and its influence on the formation of sedimentation and magmatism. The basin had undergone intense folding and faulting as understood from the number of faults, their inter-relations and relative displacements resulting into rift basins and ridges in

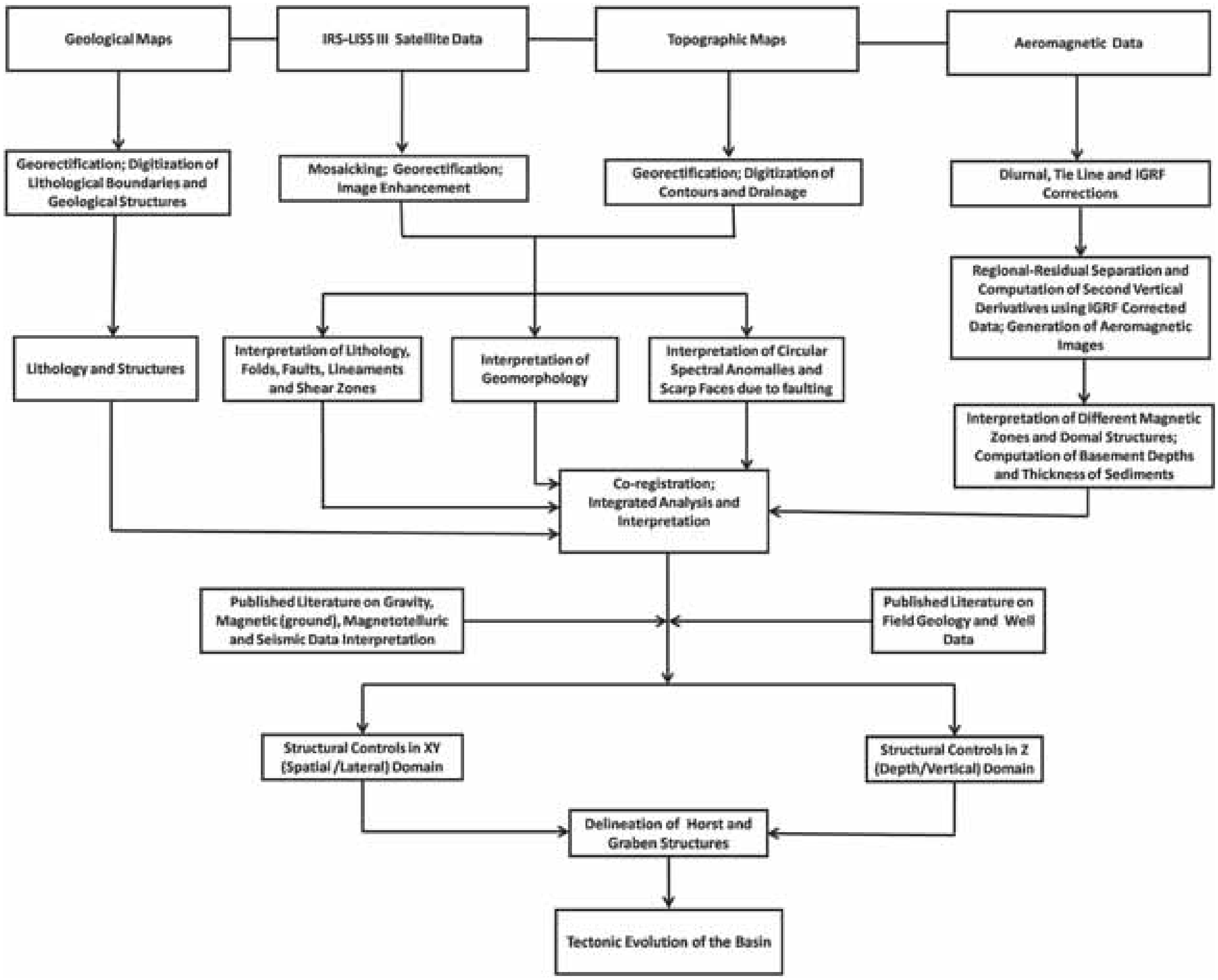

Figure 5. Methodology flowchart.

the early and middle stages of deformation and intense folding and cross folding in the terminal stages of deformation with concomitant magmatism. The whole Kutch region had experienced both horizontal and vertical tectonics in the geosynclinal environment. Hence, the interpreted structures were explained initially with emphasis on fault structures, then on fold structures and so on.

4.1 *Structures of the faulted region*

The structures of the faulted region are divided into three different categories as follows:

4.1.1 *Orthogeosynclinal stage (horizontal tectonics)*

This phase characterizes mainly horizontal movements. Analysis of satellite data shows that the development of major faults was started with the development of minor faults, and these then welded together as compound faults to form major faults at different stages, primarily in two directions – one at smaller angle (S1-sympathetic) to the applied shear direction, and the other at acute angle ($S1^1$-antithetic). Later, they had displaced each other. S1 faults are interpreted as strike-slip faults. The curvilinear strike-slip fault development and the angle between S1 and $S1^1$ faults are controlled by the pattern of shearing stress, mechanical properties of crystalline rocks and the previous structural regime. As the simple faults grow into compound faults, tensile structures like shear zones were also developed. S1 fault segments were linked up either through $S1^1$ faults or tensile structures. The compound faults exhibit many bends. The faults and fault segments inside a compound fault had stepped both right laterally and left laterally. When a right step (releasing step) is created, the fault walls were pulled apart forming ‘pull apart basins’ called ‘rhombochasm’ in parallel to the strike-slip faults such as Kutch mainland depression and Wagad depression. The left step (restraining step) had developed where the fault walls were pushed together to form the uplifts. S1 strike-slip faults are trending in nearly E–W direction, except in western part (Kutch main land) where they were observed in NNW or NW direction because of the influence of the previous synclinal structure, whereas $S1^1$ faults are steep dipping oblique faults trending in NE–SW direction at an acute angle to the strike-slip faults. It is also observed that tensional faults were developed in NW–SE direction. The intersection of the fault segments S1 and $S1^1$ had divided the whole Kutch region into parallelogram faced or rhombohedron blocks. Hence, all these blocks were bounded by the strike-slip faults or shear faults on all the sides and based on the structural relationship, some of the blocks have gone down (graben) when the releasing step conditions were satisfied and have gone up (horst) at restraining bends. These blocks are referred to as subsidence blocks/ rift blocks/rhombochasms and horsts/ridges/ uplifted blocks (Type I). Sylvester (1988) and Kusala Rajendran *et al.* (2001) were also opined on 'the strike-slip tectonics and the resulting structures' and 'the occurrence of compressional regime leading to concealed folds/faults/flexures', respectively. Basement depths and thickness of sediments computed from aeromagnetic data clearly supports this observation (Chandrasekhar *et al.* 2018). The length of the graben/depression reflects the amount of horizontal displacement and the grabens are characterised by greater depths relative to areal dimension. Depending on the depth of the basement and spacing between two parallel faults and overstep, the basin could be either rhombic in shape (Island belt zone) or parallelogram shaped with two sedimentation centers (Kutch main land) or pull aparts at terminal extension fractures (Wagad area) or series of parallel fault coalescence basins (Wagad area). Apart from the strike-slip faults shown in the maps (figures 2 and 4), two more strike-slip faults could also be expected to exist, one along the exposed Deccan trap rocks if the displaced formations including Deccan Traps to pre-Mesozoic times are rearranged, and the other one along the continental margin. The extensive emergence of magmatic activity in both effusive and intrusive forms is the characteristic feature in the development of geosynclinal region. As the ophiolitic magma activity is confined to the deep-seated faults along the subsidence, the basement has become heterogeneous (which is a characteristic feature of magnetic basement) as evidenced from aeromagnetic data interpretation (Chandrasekhar *et al.* 2018) and also supported by the interpretation of magnetotelluric data (Nagarjuna and Rao 2019). The same can be expected, even, in all the blocks of Kutch region. These subsidence zones (rhombochasms) developed in orthogeosynclinal stage have become centers for later sedimentation processes in epigeosynclinal stage. The present pattern of distribution of sedimentary basins representing the subsidence blocks (rhombochasms) show strike-slip faults on either side, trending in E–W direction as shear faults or oblique faults in NE–SW direction. The whole Kutch region, based on this study, may be divided into Kutch mainland area (Nakhtarana–Lakphat, Katrol, Bhuj and Samakhiali blocks), Banni–Lakhadia area (Banni basin, Basement ridge and Lakhadia block), East Banni–Wagad area (East Banni, Wagad and north Wagad blocks) and Island belt area (Pachham, Khadir, Bela and Chorar blocks) (Chandrasekhar *et al.* 2018).

4.1.2 *Epigeosynclinal/orogenic stage (vertical tectonics)*

This regime is mainly characterised by vertical movements (Chandrasekhar *et al.* 2018). Ravi Shanker (2001) also opined on the major faulting and rifting structures. The effect of first set of strike slip faults and high angle faults could result in 'rhombochasms' as described above. Later, the intersection of the second set of strike slip faults S2 and high angle faults S2′ (mapped from the present study) have played a key role in vertical tectonics. During this stage, the earlier formed depression in orthogeosynclinal stage which got filled up with Mesozoic sediments was subjected to deformation resulting in the upliftment of the formations to a mountainous relief. The mountainous portions in the central part of Kutch basin – Kutch mainland arch (extending from Anjar and passing through south of Bhuj, Ukhead and Rawapar, up to Lakhpat) and in the south of Wagad and Island belt were the results of the above. This deformation had also resulted in a variety of structures in the whole region; largest of them were depressions and elevations (figure 2). In the central part of the depression, smooth and gently sloping brachyformed anticlines and synclines (apart from the dome-shaped folds) are observed which reflect the block displacement of the basement. Sylvester

(1988) and An and Sammis (1996) also proposed the possibility of similar kind of structures based on their laboratory studies. Hence, the squeezed up pallial substance along the major strike-slip faults (S1 and S2) had formed well-exposed linear and folded ridges in general, followed by subsidence blocks or depressions on either side, as evidenced from remote sensing and aeromagnetic data, respectively (Chandrasekhar *et al.* 2018). The majority of the platform folds (originated in orthogeosynclinal stage) developed on the basement gradually die-out upwards along the section in sedimentary mantle. This kind of regularity becomes particularly apparent in the local elevations, which function as traps for deposits of oil and gas, perhaps indicated by the circular spectral anomalies (figures 2 and 4). Apart from the basement structures, other folded structures have also developed within the sedimentaries during further deformation. Hence, the separation of platform folds from the younger ones, according to their form and size is of significance in relation to hydrocarbon prospects. It is well known that oil and gas cannot get into the structural trap prior to formation. Thus, the time of emergence of an enclosed elevation determine the beginning of the accumulation of hydrocarbons. The duration of synsedimentary folding, its enhancement and slackening control the different phases related to the presence of hydrocarbons. The region of epi-platform activation (uplifted areas such as Kutch mainland and Wagad area) can be divided into two types. The first one is accompanied by magmatism after ending of sedimentation processes and the second one is amagmatic. Tectonic movements were characterised by a marked prevalence of intensive elevations and block displacements of the folded basement resulting in a middle and high mountainous relief in the areas separated by large depressions. During the upliftment of geosynclinal regions, longer and linear rifts with narrow width were formed under extensional regime, transverse to the direction of strike-slip faults, all along the uplifted blocks. These rift structures, in general, are the result of emergence of squeezed-up pallial substance from considerable depths. Considering the fault mechanism responsible for upliftment of the sedimentaries within the rhombochasms, another set of conjugate faults (S2-strike-slip sympathetic and $S2^1$-shear faults/high angle oblique faults – antithetic) were formed. $S2^1$ faults could have rotated $S1^1$ faults, as evidenced by the development of smaller faults and lineaments in between $S2^1$ and $S1^1$ indicating a gradual rotation (figures 2 and 4). An and Sammis (1996) also proposed similar kind of scenario. These conjugate set of faults are not only bounding earlier formed depression, but also cut across them (intra-basin faults). S2 faults are trending in ENE–WSW direction, whereas $S2^1$ faults are in NW–SE to NNW–SSE directions. The study has brought out the development of a wide shear zone in NW–SE direction in the western most part of Kutch mainland, along the eastern contact of basaltic rocks with Mesozoic sediments. This could be the typical example of reaction of competent (Deccan Trap) and incompetent (sedimentary) formations to deformation stage. Along the restraining steps (formed by the intersection of fault segments S2 and $S2^1$), sediments got uplifted, whereas along releasing steps, sediments have gone down. Maximum displacement, sometimes, can be expected near the middle of the fault segments and can go to zero at the end of the fault, probably in all the uplifted blocks. Type II pull-apart basins (Sylvester (1988) had proposed such models) and narrow and linear rift structures formed along the restraining steps all around the uplifted blocks got linked-up and, as a result, large compound basins were formed along fault trace as the fault displacements were increased further. During the two phases of deformation (magmatic and amagmatic), extrusive magmatism was predominant in the area resulting in the formation of basalts during magmatic phase. This magmatism can be expected to follow the major tectonic discontinuities such as S1 strike-slip faults. These basalts are well exposed in the western part, i.e., Kutch mainland whereas in the other areas, it might have been covered by later sediments though they were not abundant. Hence, this magmatic activity is confined mainly to the subsidence zones separating older Mesozoic sediments from the later and younger Tertiary sediments and also served as a basement for Tertiary sedimentation (Chandrasekhar *et al.* 2018). Later, all the sediments along with basaltic rocks were subjected to deformation during amagmatic phase by vertical tectonics producing a variety of folded and faulted structures. The development of narrow linear rift structures around these uplifts were noticed in Kutch mainland at the western portion of basaltic rocks hosting Tertiary sedimentation (Madh Series-9), at the eastern portion of Wagad (Khari Series-4) and in the eastern side of Kutch mainland and Bhachau and Anjar (Madh Series-9), respectively. The analysis of remote sensing and aeromagnetic data had revealed that the development of the initial rift near the uplifted margins must have followed up by parallel or ramifying rift (subsidence) structures, whose degree and extent of subsidence is lesser than that of the primary one. The same was noticed in almost all the zones in the area hosting Tertiary sedimentation. In addition, the displacements in these rift structures indicate progressive deformation. These rift structures have resulted in either 'lazy Z'-Wagad zone (NE portion of figures 1 and 2) or 'lazy S'-Kutch mainland (western portion of figures 1 and 2), which are the typical ones of Type II basins, as evidenced by the shape, size, trend, disposition and orientation of Madh and Khari series.

4.1.3 *Deltaic depression (Little Rann)*

Apart from the above, another important feature noticed in the area is triangular or delta shaped depression called 'Little Rann' (figures 2 and 4). The interpretation of IRS-LISS III data clearly shows this feature is bounded by E–W strike-slip fault on southern side, NE–SW trending fault on west and NW–SE trending fault on eastern side, respectively. Hence, this triangular depression might have originated in a similar manner either due to the upliftment of the surrounding blocks on three sides leaving the residual depression or by the subsidence along the three faults. The sporadic Mesozoic exposures within the basin were also folded with E–W axial trends. From the above analysis, it is clear that different folded and faulted structures were originated during the two stages of deformation and fault segmentation is a common phenomenon where major faults were formed by the coalescence of the simple ones. Tectonic depressions were formed where the fault segments are parallel to the plate slip-vector (releasing bends – transtension/divergent strike-slip) and uplifts occur where the fault segments are oblique to the plate slip-vector (restraining bends – transgression/convergent strike-slip). From the orientation of individual blocks, especially in the island belt area it appears that all the blocks got rotated clock-wise about the vertical axis because of the continuous shearing stress (figures 2 and 4).

4.2 *Structures of the folded region*

Numerous fold structures were also mapped from satellite data. Abrupt truncation of fold structures was also seen indicating the presence of strike-slip fault and also formation of scarp faces, alluvial fans and alluvial cones along the margins (e.g., Kutch mainland fault). The folded structures on the periphery of the subsidence blocks have often linear constitution and in the central part, brachy formed and block folds were observed. The fold structures have different orientations due to cross folding, though predominant axis is mostly E–W. Folds associated with strike-slip faults are typically arranged in enechlon pattern, oblique to the principal direction of shear and are important for hydrocarbon exploration as they form prospective traps (e.g., folds associated with the northern strike-slip fault of Kutch main land). Enechlon folds were distributed in a relatively narrow and persistent zone or adjacent to a master strike-slip fault. In addition, it is also observed that these fold patterns were distributed in very narrow zones confined by two major strike-slip faults. This enechlon pattern is most predominant along S1 or S2 trending strike-slip faults, though to a smaller extent they are also found with high angle faults. The presence of these enechlon folds represents the shortening component of the bulk strain. In three dimensions, the axial surfaces of enechlon folds in the sedimentary sequence over the rigid basement must have been nearly vertical, but higher in the overburden as they flatten upwards and twisted away from the strike of the fault and plunge away from the displacement zone (Sylvester (1988) also suggested this kind of pattern). Satellite data interpretation has shown that the enechlon folds are excellent indicators of structural development, as they reveal the following about the associated faults and related structures: (i) strike-slip fault exists either laterally or at depth, nearby, (ii) the direction of slip of the interpreted fault is in the over-stepping direction of folds, and (iii) the expected orientation of related faults. The direction of horizontal movement on the strike-slip fault is revealed by the stepping-dependant-thrusting and strike-slip faulting, which implies mechanically layered crust. It was observed that the folding was extended progressively farther away from S2 faults with increasing displacement over time. This has resulted in largest amplitude folds were at depth near the fault and the most recent folds were away from the fault and near to the margins of the deformation zone, probably represented by the circular spectral anomalies. New folds were also developed during Pliocene and Pleistocene epochs, when tectonic movements were increased, as evidenced by circular anomalies (figure 2). Circular shaped anomalies could also arise due to the subsidence along normal faults (along the axial zone of folded structure) or due to the areas of inversion, which are of gravitational origin, and expected to be connected with the flotation of the earth's crust of relatively lighter sediments such as mud saturated with gas in salt plains.

4.3 *Evolution of events*

The analysis of spatial and relational development of the structural regime had revealed the evolution of Kutch basin, sequentially, as follows: The geological evolution had initiated sometime in the Triassic period with breaking up of Gondwana land and subsequent geological history is related to northward drift of the Indian subcontinent. Mesozoic and Cenozoic tectonism related to the breaking up of the western continental margin and subsequent drift had mainly controlled the geological evolution. The drift motion and the counter-clockwise rotation could induce strike-slip movements. The rifting occurred within the weak zone of the mid-Proterozoic mobile belt by the reactivation of the pre-existing faults. The depositional history and Deccan volcanism, which rest on the southwesterly extending Proterozoic rocks are part and parcel of this major tectonic phenomenon. The Kutch rift basin originated in Triassic–early Jurassic period had formed along a reactivated movement of Delhi–Aravalli trend which swings to E–W direction in this region and had become an ideal site for Mesozoic and Cenozoic sedimentation. The other major structural trends outside the study area are Nagar Parkar uplift, Allah Bund and Sindri lake in north, Kathiawar uplift (Saurashtra horst) in south and Radhanpur–Barmer arch in east, respectively. The fold and fault patterns mapped from satellite data clearly indicate that the earth crust of this part had undergone different phases of tectonic events since Proterozoic period. The main process is geosynclinal development in different stages in certain successive order, though irregular in time and space. As such stage had developed, a comprehensive sedimentation and volcanism were localised in individual troughs (NRSA.AD.44. TR-1/1998). The basic folding is formed at the end of each stage and the most intensive magmatism is also found to be correlated with the end of each stage. The geosynclinal areas were transformed ultimately to platform regime and were subjected to horizontal and vertical movements in which vertical movements have high velocities and amplitudes. The elevations and subsidence were accompanied by fracturing of the earth's crust into separate lumps that moved at quite different rates and sometimes in different directions. The distinction in the velocities of the individual parts during orthogeosynclinal and epigeosynclinal stages became responsible for the disintegration of geosynclinal region into depressions and uplifts producing present day relief of the surface, which is the characteristic of geosynclinal regions. On the completion of geosynclinal processes, the emergence of folded region in place of geosyncline was transformed into platforms.

The causative environment for hydrocarbons and earthquakes is essentially governed by the subsurface geological structure and tectonics. This study has revealed that the sedimentary basin of Kutch is comprised of a number of sub-basins, ridges and master faults. The basins are important for hydrocarbon prospects, while the master faults are significant with regard to earthquake vulnerability. Based on this integrated study, the following four locations are recommended for hydrocarbon exploration (Chandrasekhar *et al.* 2018): (i) Banni and Samakhiali basins and north Bhuj depression; (ii) Tertiaries adjacent to strike-slip fault on the western side of Nakhtarana at a distance of 30 km; (iii) fold pattern parallel to northern boundary strike-slip fault of Kutch mainland on north of Nakhtarana at a distance of 25 km approximately; and (iv) numerous folds developed parallel to strike-slip faults in Mesozoic sediments of the northwestern portion of Anjar at a distance of 15 km to the west of Bhachau (figures 2–4). The study could also reveal that the reactivation of E–W and ENE–WSW strike-slip faults and their intersection with high angle oblique faults oriented in NW–SE and NE–SW directions could have triggered the major earthquake of Bhuj on 26th January 2001 (Chandrasekhar *et al.* 2018). All the epicenters of the aftershocks were falling in the central portion of Kutch main land, which had earlier undergone intense tectonic activity. The stress that perhaps could have caused this major earthquake may be due to the Indian plate pushing northward into Eurasian plate, resulting into reactivation of this portion of Kutch once again and subsequent re-adjustment of the basement blocks.

5. Conclusions

All the possible surface and subsurface geological structures of Kutch sedimentary basin were mapped by interpreting satellite remote sensing and aeromagnetic data, respectively. A big shear zone trending in NW–SE direction in the western portion of Kutch basin lying at the contact of Deccan Trap with Bhuj formation having a length and width of 7 km and 4 km, respectively (lying in between Valka Mota in the north and Rawapar in the south, and Nadapar in the east and Gagani in the west) was also brought out in addition to a number of fault trends. Structural controls in XY (spatial/lateral) and Z (vertical/depth) domains were derived. Regional analysis of relational displacements of different geological structures was carried out for deriving the sequence of events that occurred in the geological time scale along with tectonic movements. The results obtained were compared with published literature on gravity, magnetic (ground), magnetotelluric and seismic data, besides field geology and well data. The deformational history and tectonic evolution of the basin is understood. A conceptual tectonometamorphic model along with sedimentation and igneous activity (ophiolitic and basaltic) was thus constructed, which is capable of explaining the present day tectonic configuration of horst and graben structures hosting huge Tertiary and Mesozoic sedimentation.

Acknowledgements

We thank DGH, New Delhi for funding the aeromagnetic project. Chandra Mouli and Chandrasekhar thank Dr A Bhattacharya, Sri M Suryanarayana and Sri M V V Kamaraju, NRSC for support. Chandrasekhar thanks Director, NRSC and Head, T&ED for encouragement. Thanks are also due to the anonymous reviewers for the critical examination of the manuscript which has helped in improving the quality of the paper significantly.

References

Aitken A R and Betts P G 2008 High-resolution aeromagnetic data over central Australia assist Genville-era (1300–1100 MA), Rodinia reconstructions; *Geophys. Res. Lett.* **35** L01306.

Anand S P and Rajaram Mita 2002 Aeromagnetic data to probe the Dharwar craton; *Curr. Sci.* **83** 162–163.

Akintayo O O, Toyin O O and Adekanle O J 2014 Determination of location and depth of mineral rocks at Olode village in Ibadan, Oyo State, Nigeria using geophysical methods; *Int. J. Geophys.*, Article ID **306862**, 1–13.

Al-Nahmi F, Saddiqi O, Hilali A, Rhinane H, Baidder L, El arabi H and Khanbari K 2017 Application of remote sensing in geological mapping: Case study Al Maghrabah Area–Hajjah region, Yemen; *ISPRS Ann. Photogramm.* **IV-4/W4** 63–71.

An L J and Sammis G G 1996 Development of strike-slip faults: Shear experiments in granular materials and clay using a new technique; *J. Struct. Geol.* **8** 1061–1077.

Anudu G K, Onuba L N, Onwuemesi A G and Ikpokonte A E 2012 Analysis of aeromagnetic data over Wamba and its adjoining areas in north-central Nigeria; *Earth Sci. Res.* **16(1)** 25–33.

Babu Rao V, Atchuta Rao D, Rama Rao Ch, Sarma B S P, Bhaskara Rao D S, Veeraswamy K and Sarma M R L 1987 Some salient results of interpretation of aeromagnetic data over Cuddapah basin and adjoining terrain, south India; *Geol. Soc. India Memoir* **6** 295–312.

Berger Z, Fortin D and Wang X 2004 High-resolution aeromagnetic (HRAM) surveys: Exploration applications from the western Canada sedimentary basin – exploration in highly deformed terrains using fixed-wing aircraft and helicopter-mounted systems; *Am. Assoc. Petrol. Geol.* 40123.

Biswas S K 1971 The Miliolite rocks of Kutch and Kathiawar (Western India); *Sedim. Geol.* **5** 147–164.

Biswas S K 1974 Landscape of Kutch – A morphotectonic analysis; *Indian J. Earth Sci.* **1** 177–198.

Biswas S K 1981 Basin framework palaeoenvironment and depositional history of Mesozoic sediments of Kutch basin, western India; *QJGMM Soc. India* **53** 56–85.

Biswas S K 1982 Western rift basin of India and hydrocarbon prospects; ONGC, pp. 223–232.

Biswas S K 2005 A review of structure and tectonics of Kutch basin, western India, with special reference to earthquakes; *Curr. Sci.* **88** 1592–1600.

Biswas S K 2012 Status of petrolem exploration in India; *Proc. Indian Nat. Sci. Acad.* **78** 475–494.

Biswas S K and Deshpande S V 1973 A note on mode of eruption of Deccan Trap lavas with special reference to Kutch; *J. Geol. Soc. India* **14** 134–141.

Biswas S K and Deshpande S V 1970 Geological and tectonic maps of Kutch; *Bull. ONGC* **7** 115–116.

Biswas S K and Deshpande S V 1968 Basement of the Mesozoic sediments of Kutch, western India; *Bull. Geol. Min. Met. Soc. India* **40** 1–7.

Blakely R J 1995 *Potential Theory in Gravity and Magnetic Applications*; Cambridge University Press, Cambridge, 441p.

Boyd D M and Isles D J 2007 Geological interpretation of airborne magnetic surveys-40 years on; In: *Proceedings of Exploration 07: Fifth Decennial International Conference on Mineral Exploration* (ed.) B Milkereit, pp. 491–505.

Boyd D 1969 The contribution of airborne magnetic survey to geological mapping, mining and groundwater geophysics 1967; *Geol. Survey Canada, Econ. Geol. Rep.* **26** 213–227.

Chandrasekhar D V, Singh B, Firozishah M and Mishra D C 2005 Analysis of gravity and magnetic anomalies of Kachchh rift basin, India and its comparison with the New Madrid seismic zone, USA; *Curr. Sci.* **88** 1601–1608.

Chandrasekhar P, Chandra Mouli K, Rao D P and Dadhwal V K 2018 Subsurface geological structure and tectonics as evidenced from integrated interpretation of aeromagnetic and remote sensing data over Kutch sedimentary basin, western India; *Curr. Sci.* **114** 174–185.

Chandrasekhar P and Seshadri K 2013 Analysis of remote sensing and aeromagnetic data for identification of the causative factors for the recent micro-seismicity observed in Vanasthalipuram area of Ranga Reddy district, Andhra Pradesh, India; *Curr. Sci.* **104** 502–508.

Chandrasekhar P, Tapas R M, Venkateswarlu N, Subramanian S K and Kamaraju M V V 2011 Regional geological studies over parts of Deccan syneclise using remote sensing and geophysical data for understanding hydrocarbon prospects; *Curr. Sci.* **100** 95–99.

Chandrasekhar P 2010 Integration of high resolution satellite data and electrical resistivity technique for groundwater exploration and exploitation over parts of Mahbubnagar district, A.P., India; *J. Ind. Geophys. Union* **14** 211–218.

Chandrasekhar P, Vinod Kumar K, Tapas R M and Subramanian S K 2009 Multi-Earth observation data to identify indicators for mineralized zones in parts of Iran; *J. Ind. Geophys. Union* **13** 133–138.

Colin Reeves 2005 Aeromagnetic Surveys: Principles, Practice and Interpretation; *Published by GEOSOFT*, 155p.

Cowan and Cowan 1991 Analytical techniques in interpretation of aeromagnetic data; *Explor. Geophys.* **22** 81–84.

Das S, Pardeshi S D, Kulkarni P P and Doke A 2018 Extraction of lineaments from different azimuth angles using geospatial techniques: A case study of Pravara basin, Maharashtra, India; *Arab. J. Geosci.* **11** 160.

David J I and Leigh R R 2013 *Geological interpretation of Aeromagnetic data*; Australian Society of Exploration Geophysicists, 357p.

Deshpande S V 1982 Precambrian basement configuration of Saurashtra peninsula, W. India; Abstract, *Proc. Symp. Indian Lithosphere*.

Ganguly K and Mitran T 2016 Delineation and assessment of Central Indian Suture through lineament extraction approach using remote sensing and geographic information system; *Geocarto Int.* **31** 308–327.

Gaonkar S G 2003 Study of the epicentral trends and depth sections for aftershocks of the 26th January 2001, Bhuj earthquake in western India; *Proc. Indian Acad. Sci. (Earth Planet. Sci.)* **112** 401–412.

Ghosh D and Ramesh Acharya G 2006 Structural features of Bundelkhand granite complex for geology and structure; *J. Geol. Soc. India* **68** 949–958.

Hinze W J and Zietz I 1985 *The composite magnetic anomaly map of the conterminous United States: The utility of regional gravity and magnetic anomaly maps* (ed.) Hinze W J, Soc. Expl. Geophysicists.

Kusala Rajendran, Rajendran C P, Mahesh T and Martitia P T 2001 The 2001 Kutch (Bhuj) earthquake: Coseismic surface features and their significance; *Curr. Sci.* **80** 1397–1405.

Masoud A A and Koike K 2011 Morphotectonics inferred from the analysis of topographic lineaments auto-detected from DEM: Application and validation for the Sinai peninsula, Egypt; *Tectonophys.* **510** 291–308.

Mathew M P, Ramachandra H M, Gouda H C, Singh R K, Ramesh Acharya G, Murthy Ch V V S and Rao K S 2001 IGRF corrected regional aeromagnetic anomaly map of parts of peninsular India – Potential for mapping and mineral exploration; *GSI Spec. Publ.* **58** 395–406.

Merh S S 1995 Geology of Gujarat; Geol. Soc. India.

Mikhailov A Ye 1987 *A Text Book on Structural Geology and Geological Mapping*; Mir Publishers, Moscow, 535p.

Milligan P R and Gunn P J 1997 Enhancement and presentation of airborne geophysical data; *AGSO J. Austr. Geol. Geophys.***17** 63–75.

Mishra D C, Arora K and Tiwari V M 2004 Gravity anomalies and associated tectonic features over the Indian Peninsular Shield and adjoining ocean basins; *Tectonophys.* **379** 61–76.

Mishra D C, Chandrasekhar D V and Singh B 2005 Tectonics and crustal structures related to Bhuj earthquake of January 26, 2001 based on gravity and magnetic surveys constrained from seismic and seismological studies; *Tectonophys.* **396** 195–207.

Misra K S, Bhutani R and Sonp R 2003 Aftershocks of 26th January 2001 Bhuj earthquake and seismotectonics of the Kutch region; *Proc. Indian Acad. Sci. (Earth Planet. Sci.)* **112** 385–390.

Murthy B S R 2007 Airborne geophysics and the Indian scenario; *J. Indian Geophys. Union* **11** 1–28.

Nagarjuna D and Rao C K 2019 Magnetotelluric study to characterize sediment thickness across Kachchh and Cambay rift basins, western India; *Curr. Sci.* **116** 299–304.

NRSA Tech. Rep. No. NRSA.AD.44.TR-1/1998 Aeromagnetic survey–Interpretation with IRS data in structural mapping for hydrocarbon exploration over Kutch Basin, Gujarat, 112p.

Prasanti Lakshmi M and Ram Babu H V 2002 Basement structure of the southwestern part of the Cuddapah Basin from aeromagnetic anomalies; *Curr. Sci.* **82** 1378–1381.

Radhakrishna Murthy I V 1992 Magnetic interpretation in space domain, Second SERC School on Geomagnetism and Earth's Interior-Geopotentials-1, Sponsored by the Department of Science and Technology, New Delhi; Lecture Notes. pp. 33–62.

Rajaram M, Anand S P and Balakrishna T S 2006 Composite magnetic anomaly map of India and its contiguous regions; *J. Geol. Soc. India* **68** 569–576.

Rajaram Mita and Anand S P 2003 Central Indian tectonics revisited using aeromagnetic data; *Earth Planet. Space* **55** 1–4.

Rajendra Sarma, Murthy Ch V V S, Gouda H C and Singh R K 2006 Analysis of aeromagnetic data over part of Bundelkhand Granite Complex delineated by aeromagnetic expression around Jhansi, Uttar Pradesh; *J. Geol. Soc. India* **68** 949–958.

Ramachandra H M, Mathew M P, Ramesh Acharya G, Gouda H C and Singh R K 2001 Aeromagnetic anomaly interpretation and correlation with geological features of Central India; *GSI Spec. Publ.* **64** 163–176.

Rama Rao B S and Murthy I V R 1978 *Gravity and Magnetic Methods of Prospecting*; Arnold–Heinemann Publications, pp. 285–353.

Rao D A and Babu H V R 1984 On the half-slope and straight-slope methods of basement depths determination; *Geophysics* **49** 1365–1368.

Rao D P, Bhattacharya A and Reddy P R 1996 Use of IRS-1C data for geological and geographical studies; *Curr. Sci.* **70** 619–623.

Rao D P, Bhattacharya A, Navalgund R R, Sengupta S, Roy A K, Bhanu Masthan, Hegde V S and Suryanarayana M 1992 Oil field detection through remote sensing; *NRSA Technical Report,* 11p.

Ravi Shanker 2001 Seismotectonics of Kutch rift basin and its bearing on the Himalayan seismicity; *ISET J. Earthq. Technol.* **38** 59–65.

Reddy A G B, Mathew M P, Baldau Singh and Naidu P S 1988 Aeromagnetic evidence of crustal structure in the granulite terrain of Tamil Nadu, Kerala; *J. Geol. Soc. India* **32** 368–381.

Reeves C V 1992 New Horizons in airborne geophysical mapping; *Expl. Geophys.* **23** 273–280.

Reeves C V 1994 Towards a magnetic anomaly map of reconstructed gondwana; *Ninth International Gondwana Symposium* **2** 963–969.

Reid A B, Allsop J M, Gransee H, Millet A J and Somerton I W 1990 Magnetic interpretation in three dimensions using Euler deconvolution; *Geophysics* **55** 80–91.

Seshadri K and Chandrasekhar P 2013 Identification of groundwater potential locations using high-resolution satellite data in a densely populated urban area of greater Hyderabad city, Andhra Pradesh, India; *J. Ind. Geophys. Union* **17** 409–416.

Seshavataram B T V 2016 *Offshore sedimentary basins of India: Geology, tectonics and hydrocarbon prospects*; BS Publications, 210p.

Sreedhar Ganapuram, Vijaya Kumar G T, Murali Krishna I V, Ercan Kahya and Cuneyd Demirel M 2009 Mapping of groundwater potential zones in the Musi basin using remote sensing data and GIS; Adv. Eng. Software, Elsevier **40** 506–518.

Sumer Chopra K, Madhusudhan Rao and Bharati K Rastogi 2010 Estimation of sedimentary thickness in Kachchh Basin, Gujarat using Sp converted phase; *Pure Appl. Geophys.* **167(10)** 1247–1257.

Suryanarayana M, Bhattacharya A and Rao D P 1992 Image processing of aeromagnetic data and its integration with satellite image for improved geological interpretation – A case study of Orissa, India; *J. Assoc. Expl. Geophys.* **XIII 3** 117–124.

Sylvester A G 1988 Strike Slip faults; *Geol. Soc. Am. Bull.* **100** 1666–1703.

Thakkar M G 2017 *Geomorphological Field Guide Book on Kachchh Peninsula* (ed.) Amal Kar, Indian Institute of Geomorphologists, Allahabad.

Willian S K and Willian E G 1987 Image processing of aeromagnetic data and integration with Landsat images for improved structural interpretation; *ITC Journal* **4** 305–313.

Zonenshain L P, Verhoef J, MacNab R and Meyers H 1991 Magnetic imprints of continental accretion in the USSR; *EOS.* **72** 305–310.

Corresponding editor: ARKOPROVO BISWAS